A R C H I V E S O F M E T A L L U R G Y A N D M A T E R I A L S
Volume 50 2005 Issue 3

M. JANUS-MICHALSKA*

EFFECTIVE MODELS DESCRIBING ELASTIC BEHAVIOUR OF CELLULAR MATERIALS

MODEL EFEKTYWNY MATERIAŁÓW KOMÓRKOWYCH W ZAKRESIE LINIOWO-SPRĘŻYSTYM

The aim of this paper is to formulate an effective anisotropic continuum for cellular materials based on micromechanical modeling. It corresponds to recent trend, of searching for advanced materials tailored to special requirements, which is based on intrinsic relation between structure and macroscopic properties. Open-cell materials with diverse structures representing different types of symmetries are considered. It is assumed that essential macroscopic features of mechanical behaviour can be inferred from the deformation response of a representative volume element. The structural mechanics methods are applied for a beam model of skeleton. An analytical formulation of force-displacement relations for the skeleton struts is found by considering the affinity of nodal displacement in tensile, bending and shear deformations. The concept of multiscale modeling leads to formulation of equivalent continuum as an effective model. Such an approach is typical for micromechanics. The stiffness tensor may be produced for anisotropic solid depending on material properties of the solid phase and topological arrangement of a cellular structure using the micro-macro transition. The analysis based on the assumption of linear elasticity leads to the analytical solution. Graphical representation of choosen material constants is performed. The possibility to model the influence of morphology and topology parameters is studied.
The proposed theoretical framework of micromechanical modeling can be extended to nonlinear behaviour, plasticity and failure analysis. For such problems numerical approach is required.

Keywords: cellular materials, anisotropy, effective model, micromechanical modeling, elasticity

Poszukiwanie nowych wielofunkcyjnych materiałów odpowiada najnowszym tendencjom tworzenia materiałów o założonych z góry własnościach w tym również własnościach mechanicznych. Takie modelowanie oparte jest na znajomości relacji pomiędzy strukturą

* INSTITUTE OF STRUCTURAL MECHANICS, CRACOW UNIVERSITY OF TECHNOLOGY, 31-155 KRAKOW, UL. WARSZAWSKA 24, POLAND

wewnętrzną a własnościami materiału w skali makro. Ustalenie tych relacji jest podstawowym zadaniem, którego rozwiązanie prowadzi do skonstruowania modelu efektywnego.

Obiektem rozważań są materiały komórkowe o komórkach otwartych, które tworzą szkielet mikrostruktury o regularnym przestrzennym układzie oraz pianki charakteryzujące się układem nieregularnym. Własności mechaniczne takich struktur można wyznaczyć w oparciu o szczegółową analizę komórki reprezentatywnej, z postaci której można wnioskować o symetrii materiału. W pracy zastosowano typową dla mikromechaniki koncepcję modelowania dwuskalowego, która prowadzi do sformułowania continuum zastępczego jako modelu efektywnego. Analizę kinematyczną w strukturze przeprowadzono przy spostrzeżeniu podobieństwa przemieszczeń względnych komórek dla jednorodnych stanów odkształceń materiału w skali makro. Szkielet struktury modelowano jako belkę Timoshenki wyprowadzając relacje siła-przemieszczenie w szkielecie poprzez sztywności osiowe i giętne belek. Dla określenia naprężenia efektywnego continuum zastosowano definicje uśrednionych naprężeń rzeczywistych w szkielecie. Powyższy algorytm pozwala wyznaczyć składowe tensora sztywności dla materiału anizotropowego jako funkcje sztywności elementów składowych i parametrów opisujących geometrię komórki reprezentatywnej.

Praca zawiera prezentację graficzną wybranych stałych materiałowych dla poszczególnych struktur ze wskazaniem na możliwość modelowania wskazanych własności sprężystych materiału.

1. Introduction

Highly porous materials with cellular structure exhibit many interesting combinations of physical and mechanical properties such as high stiffness in conjunction with very low specific weight. For this reason they are frequently used to fulfill constructional and functional purposes. The development of mechanics of cellular solids is documented by Gibson and Ashby [1]. Banhart [2] gives detailed description of manufacturing possibilities and diversity of applications. Cellular materials are finding an increasing range of applications in light-weight construction, crash energy absorption, aerospace industry, shipbuilding, sporting equipment, biomedical industry. These materials also exhibit properties which suggest their implementation as multifunctional materials [3] for such applications as cooling devices, heat exchangers, silencers, filtration, transfer of liquid, flame arresters, acoustic control. Cellular solids are materials made up of an interconnected network of cells with solid strut edges. The cell faces can be open or covered by plates or membranes. Distinction is made between open and closed cell materials, which are inherently different. Searching for new multifunctional materials corresponds to recent trend of searching for advanced materials tailored to special requirements [4, 5, 6]. The empirical development of such materials by trial and error may be very time consuming and expensive. An essential step toward implementation comprises structural analysis. Advanced modeling of materials relies on the intrinsic relation between structure and properties. Establishing this relation is a challenge for researches. Fundamental studies of phenomena on a micro-scale are necessary to explain the macroscopic behaviour of such structured bodies. The overall effective properties are determined by certain considerations using micro-macro transition. It is related to effective model construction [7, 8, 9]. The effective properties are then

used to determine the response of structural elements on a macro scale and emerge naturally as a consequence of micro-macro relations without depending on specific physical measurements [8]. This method, typical for micromechanics, has been applied to aluminum foams [10].

2. Micromechanical analysis

2.1. Representative unit cells for different microstructures

Our interest is focused on typical cellular materials with skeleton structures shown in Fig. 1.

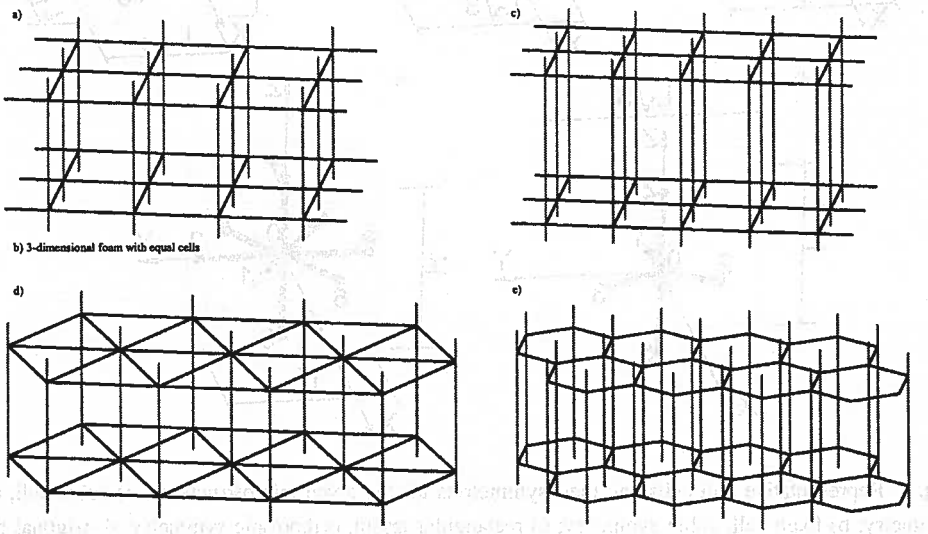

Fig. 1. Examples of 3-D cellular structures, which may be described by the present formulation

Formulation on a micro level begins by identifying the unit cell of the spatially periodic array or volume. Thin lines identify the volume within the symmetry planes surrounding the part of the skeleton (thick line) inside the unit cell. Unit cells have the property of filling space by appropriate repetitions of themselves when mirrored and inverted about the faces of the element in all directions without introducing gaps or overlaps. Cells satisfying these conditions composed of four, six or eight members converging into a node (rigid joint) with the description of cell geometries are shown in Fig. 2. These unit cells correspond to structures given in Fig. 1.

An open-cell microstructure is represented by unit cell with a part of skeleton having half struts of length $L_{0-i}/2$. The unit cell position is considered with respect to the assumed coordinate system having the origin at vertex 0. The strut midpoints are

described by the position vectors $\mathbf{b}_i^0 i = 1,....n$ where: $|\mathbf{b}_i^0| = {}^{L_{0-i}}/_2$. Representative volume element V has face areas A_i perpendicular to struts i.

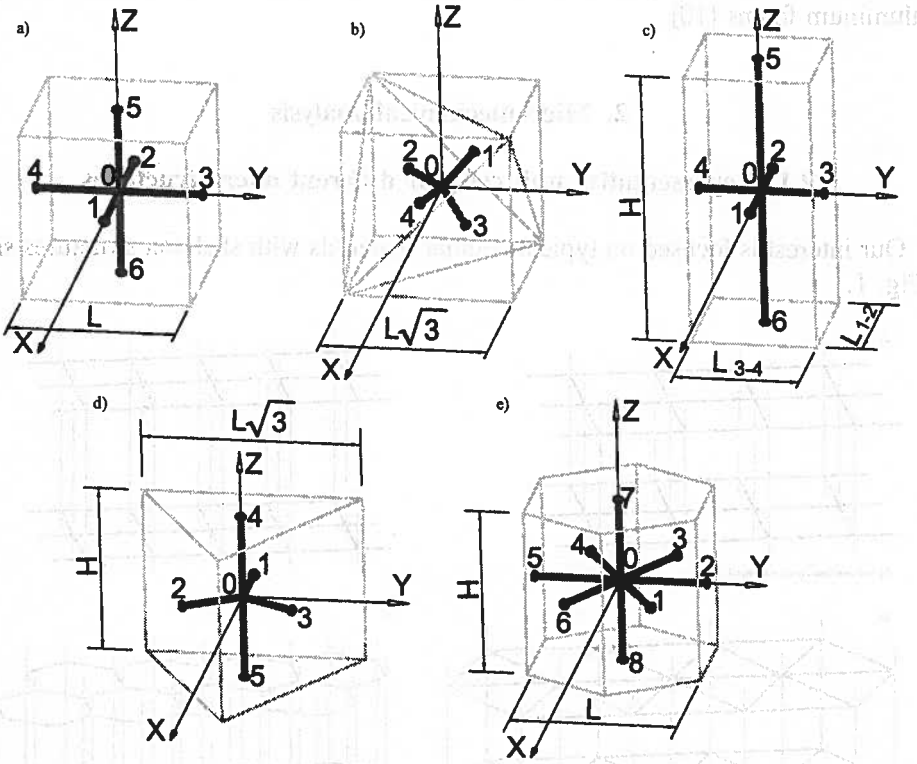

Fig. 2. Representative unit cells and their symmetries for the given microstructures: a) cubic cell, cubic symmetry; b) foam cell, cubic symmetry; c) rectangular prism, orthotropic symmetry; d) trigonal prism, transversely isotropic symmetry; e) hexagonal prism, transversely isotropic symmetry

2.2. Strain and stress measures for linear elasticity

The unit cell is treated as a model on the basis of which effective relations between strains and stresses are established. These strains and stresses are defined as volumetric averages of the micro field variables [8], which are defined as given below:

$$\boldsymbol{\varepsilon} = \langle \boldsymbol{\varepsilon}^s \rangle_V = \frac{1}{V} \sum_{A_i} sym\,(\mathbf{n}_i \otimes \mathbf{u}_i) dS, \qquad \boldsymbol{\sigma} = \langle \boldsymbol{\sigma}^s \rangle_V = \frac{1}{V} \sum_{A_i} (\mathbf{t}_i \otimes \mathbf{n}_i) dS \qquad (1)$$

where: $\langle\rangle_V$ stands for the volumetric average in skeleton s taken over V, $\mathbf{n}_i$ is the outer unit normal on the boundary A_i and $\mathbf{u}_i$ and $\mathbf{t}_i$ are respectively the midpoint displacement on the surface A_i and surface traction defined as follows: $t_i = {}^{F_i}/_{A_i}$.

This means that strains and stresses are measured using the unit cell's surface displacements and tractions, respectively.
A representative volume element with its mechanical model is used to determine the effective properties using the principles mentioned above on a micro-scale together with the assumption of uniform strain and stress state.

2.3. Kinematics

The essential feature of uniform deformation of solids with repetitive microstructure is node displacement affinity. The spatially periodic nature of the cell array requires that the individual beams deform antisymmetrically about their midpoints, so there is no resultant moment across the section at the beam midpoints. An example of such deformation is shown in Fig. 3.

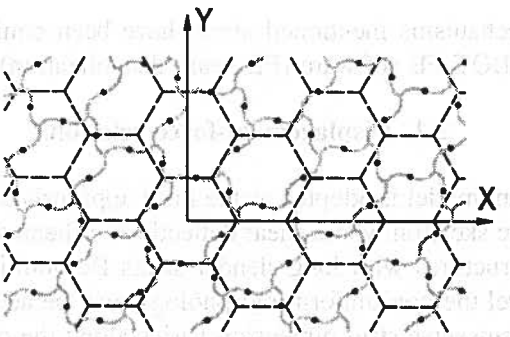

Fig. 3. Example of uniform deformation

The kinematics of the unit cell is described by the relative displacements of the beam midpoints with respect to a rigid motion of the junction point (vertex). This rigid motion is described by the translation component Δ_0 and spatial rotation Ψ. As a result relative midpoint displacement with respect to node is given by the following formula:

$$\Delta_{i-0} = \Delta_i - \Delta_0 - \Psi \times \mathbf{b}_0 \qquad i = 1, ...n. \tag{2}$$

Note that only this relative deformation produces forces in microstructure skeleton. The uniform axial deformation results in the motion of the beam midpoints which may be described as written below:

$$\Delta_i(\varepsilon_\alpha) = \varepsilon_\alpha \cdot \left(\mathbf{b}_i^0 \cdot \mathbf{e}_\alpha\right) \mathbf{e}_\alpha \qquad i = 1, ...n \tag{3}$$

for subsequent uniaxial extensions ε_α in the α direction $\alpha = x, y, z$.

For pure shearing deformation in the $\alpha\beta$ plane $\alpha \neq \beta$ the displacements are given as follows:

$$\Delta_i\left(\gamma_{\alpha\beta}/2\right) = \left(\gamma_{\alpha\beta}/2\right) \cdot \left(\left(\mathbf{b}_i^0 \cdot \mathbf{e}_\alpha\right) \mathbf{e}_\beta + \left(\mathbf{b}_i^0 \cdot \mathbf{e}_\beta\right) \mathbf{e}_\alpha\right) \qquad i = 1, ...n. \tag{4}$$

The location and rotation of the junction point is determined by enforcing cell equilibrium:

$$\sum_{i=1}^{n} \mathbf{F}_i = 0 \qquad \sum_{i=1}^{n} \mathbf{F}_i \times \mathbf{b}_i^0 = 0. \tag{5}$$

Relative displacements may be represented by the components normal and tangent to the individual strut direction

$$\Delta_{0-i} = \Delta_{0-i,n} + \Delta_{0-i,\tau}, \tag{6}$$

where displacement components can be obtained using the following formula:

$$\Delta_{0-i,n} = (\Delta_{0-i} \cdot \boldsymbol{e}_i)\, \mathbf{e}_i \qquad \Delta_{0-i,\tau} = (\mathbf{e}_i \times \Delta_{0-i}) \times \mathbf{e}_i. \tag{7}$$

The deformation mechanisms mentioned above have been confirmed by calculations performed using ROBOT FE software (FE beam discretization).

2.4. Displacement-force relations

Timoshenko beam model is adopted as the most appropriate for short beams of the typical microstructure skeleton where shear deflections of beams should be considered. For a low density structures with long slender struts Bernoulli-Euler beam theory is sufficient. At this level the non-uniform morphology may be accounted for. It refers to the case where the transverse strut dimension varies along the centerline axis with the maximum value at the joint to the minimum at the midpoint.

The elastic behaviour of cantilever beam subject to axial and transverse loads is known from classical solutions. The appropriate differential equations together with boundary conditions are quoted in [10].

For axial load F_{in} and transversal load $F_{i\tau}$, applied at the end of cantilevered beam, its free end axial displacement $\Delta_{i-0,n}$ and transversal displacement $\Delta_{i-0,\tau}$ may be described by linear relations with respect to fixed end:

$$\Delta_{0-i,n} = F_{in} c_{in} \qquad \Delta_{0-i,\tau} = F_{i\tau} c_{i\tau}, \tag{8}$$

where: c_{in} is defined as beam axial elastic compliance of strut i

$c_{i\tau}$ is defined as bending elastic compliance of strut i having the length $L_{0-i}/2$.

For uniform beam cross-section the solutions are as follows:

$$c_{in} = \frac{L_{0-i}}{2E_S A} \qquad c_{i\tau} = \frac{L_{0-i}^3}{24E_S J} + \frac{L_{0-i}}{2G_S A_\tau}, \tag{9}$$

where: A — cross-sectional area

$E_s G_s$ — Young and shear modulus for the skeleton material.

For slender strut modeled using the Bernoulli-Euler beam model deflection depends

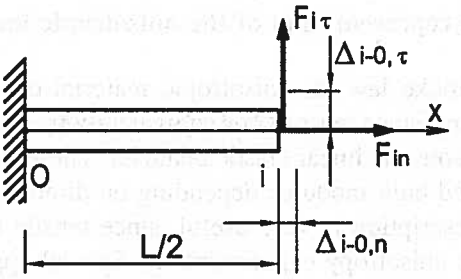

Fig. 4. Cantilevered beam representing microstructural element

only on distribution of bending moments. For Timoshenko beam additional displacement component related to shearing stress should be included. It may be determined by solving equations quoted in [10]. For such a model bending elastic compliance is a sum of two components. The first one corresponds to Bernoulli-Euler beam response whereas the second one is related to shearing strains present in Timoshenko beam.

For nonuniform cross-section elastic beam compliances are functions of microstructure morphology.

Axial and bending stiffnesses of beams are given by inverts of compliances:

$$s_{in} = (c_{in})^{-1}, \qquad s_{i\tau} = (c_{i\tau})^{-1}. \tag{10}$$

When the stiffnesses are determined, one may calculate the normal and transversal forces as functions of unknown nodal rigid motions using force-displacement relations. The displacement and rotation components may be obtained from equilibrium equations (5). The solution supplies full description of deformation mechanism.

2.5. Effective elasticity tensors

The forces obtained in such a way make the calculation of stresses in an equivalent continuum possible following the definition (1). Six types of specific deformations related to subsequent strain tensor components being non zero one at a time are considered (3), (4). As a result of the analysis the effective constitutive matrix for the unit cell is constructed.

For the given types of symmetries the elasticity tensors in Kelvin notation [11, 12] are given in Appendix.

Nonzero components of elasticity tensor are given in Table 1. Generally theses components are functions of structural element stiffnesses and geometrical parameters of representative volume elements.

Note that the effective properties are dependent not only on relative density but also on strut morphology both in cross-section and variation along the strut length.

All the obtained results are compatible with those available in literature [19].

3. Graphical representation of the anisotropic linear properties

The generalized Hooke law for anisotropic material can be given by 4-th order stiffness tensor **S** or compliance tensor **C** or equivalently by two scalar functions, which uniquely determine anisotropic linear elastic behavior. These functions represent Young modulus and generalized bulk modulus depending on direction of tension in a tension test [15]. This latter description is very useful, since tensile test is the most frequent test determining elastic anisotropy experimentally. Special applicability of anisotropic materials requires the capability to visualize their properties. All directions in $\mathfrak{R}^3$ can be parametrized by spherical coordinates $\{r, \varphi, \vartheta\}$ with $r = 1$. Young modulus or generalized bulk modulus can be effectively represented by means of spherical polar diagram, i.e. with a surface generated by a vector whose length is proportional to the value of modulus in the direction indicated by the vector itself.
Since the dependence of macroscopic properties on Young modulus of the skeleton material is linear it is useful to show dimensionless plots.
For properties such as shear modulus and Poisson's ratio only planar representation is possible and it is drawn in chosen planes.
Geometric parameters of skeleton structure are chosen in a way that avoids buckling (struts are not overly slender) and Timoshenko beam theory is valid (struts are not overly thick).

3.1. Young's modulus and generalized bulk modulus

A tensile test is represented by an uniaxial stress state having tensile direction **n**. Young modulus $E(\mathbf{n})$ definition as the ratio of tensile stress to tensile strain leads to the following formula [12, 15]:

$$\frac{1}{E(\mathbf{n})} = (\mathbf{n} \otimes \mathbf{n}) \cdot \mathbf{C} \cdot (\mathbf{n} \otimes \mathbf{n}), \tag{11}$$

where: **n** normalized vector specyfing the tensile direction in a tension test

Note that the expression $\frac{1}{E(\mathbf{n})}$ corresponds to elastic energy [14] stored in a body subject to uniaxial stress state of a unit value. This allows for the interpretation of the directions corresponding to extremes of Young's modulus as directions of maxima and minima for the stored energy function. Maxima are oriented along directions parallel to the skeleton struts as a consequence of axial stiffness exceeding the bending stiffness in structural elements.

Calculations are performed for the following geometric data:
a) $L = 1.5 * 10^{-4}m$, $R = 9.375 * 10^{-6}m$
b) $L = 1.5 * 10^{-4}m$, $R = 1.0 * 10^{-5}m$
c) $L_{1-2} = 1.5 * 10^{-4}m$, $L_{3-4} = 2.55 * 10^{-4}m$, $H = 2.7 * 10^{-4}m$, $R = 1.37 * 10^{-5}m$
d) thick structure: $L = 1.5 * 10^{-4}m$, $H = 2.0 * 10^{-4}m$, $R = 1.35 * 10^{-5}m$

d) slender structure: $L = 1.5 * 10^{-4}m$, $H = 2.0 * 10^{-4}m$, $R = 0.5 * 10^{-5}m$
e) $L = 1.5 * 10^{-4}m$, $H = 2.0 * 10^{-4}m$, $R = 1.35 * 10^{-5}m$
where: R is radius of the uniform circular beam cross-section.
It yields the plots presented in Fig. 5.

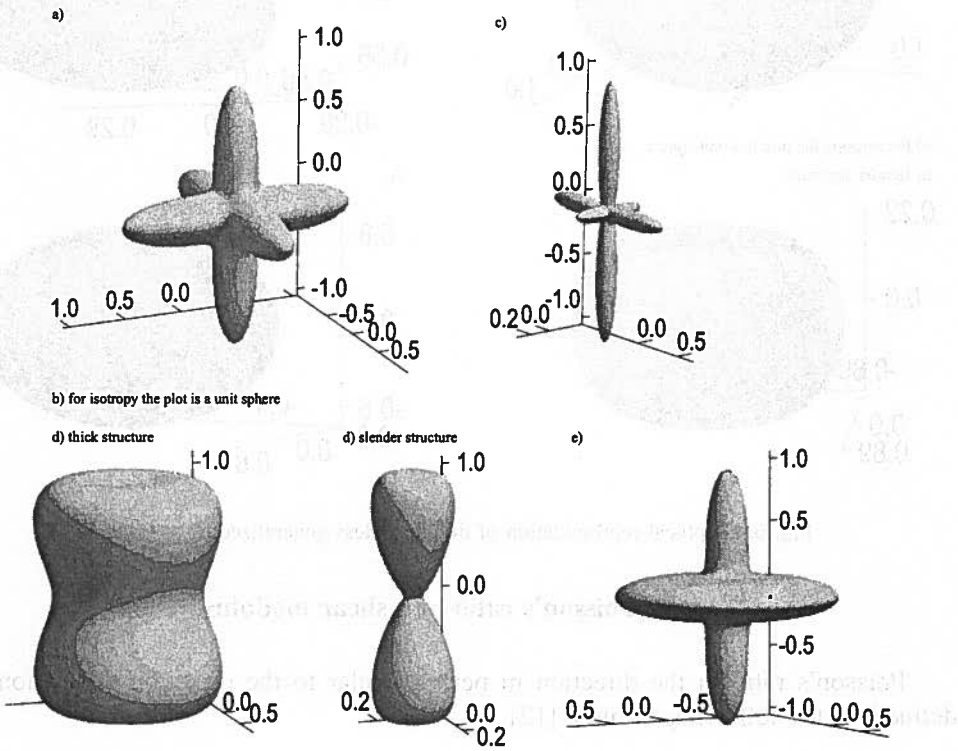

Fig. 5. Graphical representation of dimensionless Young's moduli

Generalized bulk modulus $K(\mathbf{n})$ is defined as one third of the ratio of a tensile stress and the trace of the strain tensor [15]. The quantity $\frac{1}{3K(\mathbf{n})}$ represents the relative change of volume per tensile unit stress in the direction $\mathbf{n}$ and can be obtained using the following formula:

$$\frac{1}{3K(\mathbf{n})} = \mathbf{I} \cdot \mathbf{C} \cdot (\mathbf{n} \otimes \mathbf{n}). \tag{12}$$

Calculations are performed for the same geometric and material data as previously. It gives the plots presented in Fig. 6.

Minima are directed along directions parallel to the skeleton struts as a consequence of axial stiffness being greater than bending stiffness for structural elements.

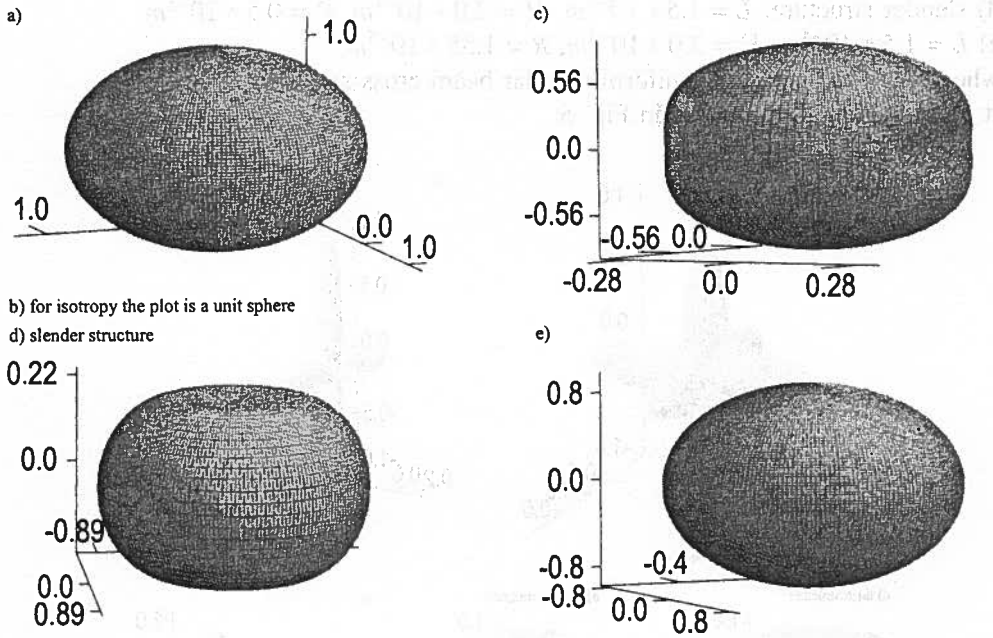

Fig. 6. Graphical representation of dimensionless generalized bulk moduli

3.2. Poisson's ratio and shear modulus

Poisson's ratio in the direction m perpendicular to the direction of tension n is defined by the following formula [12]:

$$\frac{-\nu(\mathbf{n},\mathbf{m})}{E(\mathbf{n})} = (\mathbf{n}\otimes\mathbf{n})\cdot\mathbf{C}\cdot(\mathbf{m}\otimes\mathbf{m}). \tag{13}$$

Considerations in xy plane for a honeycomb made of square or rectangular cells, yields a plot typical for all structures in xz or yz planes. For structures d) and e) the plot is circular as can be expected for transversal anisotropy. Since the typical honeycomb d) is more compliant, its Poisson's ratio is greater than for honeycomb e).

Calculations are performed for data given previously.

Shear modulus for two perpendicular directions can be obtained by the formula:

$$\frac{1}{2G(\mathbf{n})} = (\mathbf{n}\otimes\mathbf{m})\cdot\mathbf{C}\cdot(\mathbf{n}\otimes\mathbf{m}). \tag{14}$$

Plots for similar cases as for Poisson's ratio are given in Fig. 8.

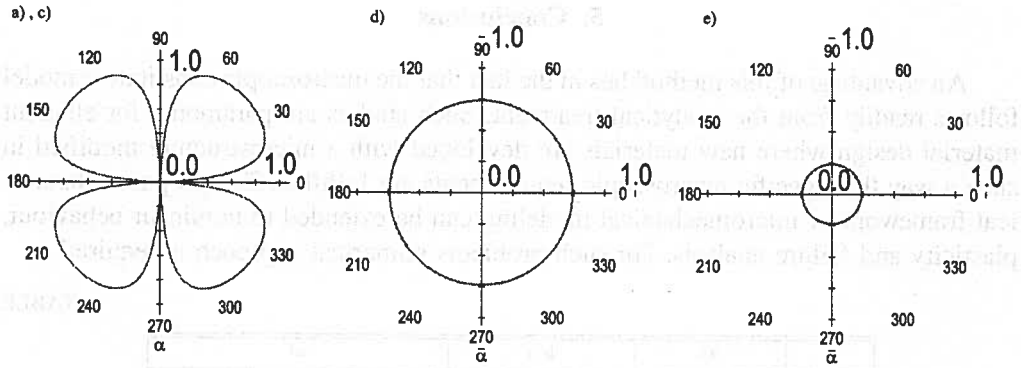

Fig. 7. Graphical representation of Poisson's ratio for XY plane (α is defined as angle with direction n)

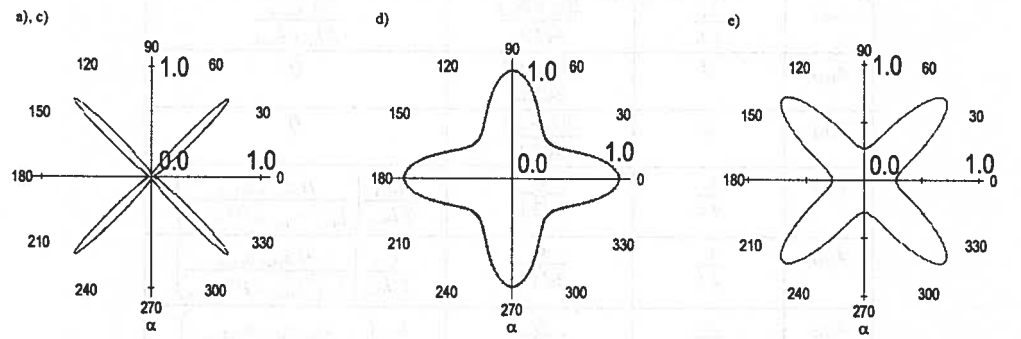

Fig. 8. Graphical representation of shear modulus plane (α is defined as angle with direction n), a)XY plane, d)e) XZ plane

4. The topological design

Detailed study based on described examples leads to the conclusion, that responses in skeleton structure are fundamentally related to bending and stretching deformations. Cellular systems that bend are subject to high local stresses which make the system compliant and result in low yield strength. Conversely when the cell walls stretch without bending the system is stiff and exhibits high strength. Thus, from the structural perspective skeleton structure of the type e) is by far superior to all other configurations, since only it works during shearing deformation without bending of structural elements. Skeleton structure of the type d) is very compliant because bending occurs during every possible uniform deformation.

Topological design including the choice of microstructure type is responsible for macroscopic distribution and directional dependence of properties.

5. Conclusions

An advantage of this method lies in the fact that the macroscopic constitutive model follows readily from the analytical treatment. Such studies are paramount for efficient material design where new materials are developed with a microstructure modified in such a way that specific macroscopic requirements are fulfilled. The proposed theoretical framework of micromechanical modeling can be extended to nonlinear behaviour, plasticity and failure analysis. For such problems numerical approach is required.

TABLE

	a)	b*)	c)
s_{1111}	$\frac{s_n}{2L}$	$\frac{2(s_n+2s_\tau)}{9\sqrt{3}L}$	$\frac{L_{1-2}\,s_{n1-2}}{2\,L_{3-4}\,H}$
s_{2222}	$\frac{s_n}{2L}$	$\frac{2(s_n+2s_\tau)}{9\sqrt{3}L}$	$\frac{L_{3-4}\,s_{n3-4}}{2\,L_{1-2}\,H}$
s_{3333}	$\frac{s_n}{2L}$	$\frac{2(s_n+2s_\tau)}{9\sqrt{3}L}$	$\frac{H\,s_{n5-6}}{2\,L_{1-2}\,L_{3-4}}$
s_{1122}	0	$\frac{2(s_n-s_\tau)}{9\sqrt{3}L}$	0
s_{1133}	0	$\frac{2(s_n-s_\tau)}{9\sqrt{3}L}$	0
s_{2323}	$\frac{s_\tau}{4L}$	$\frac{s_\tau}{3\sqrt{3}L}$	$\frac{L_{3-4}}{2\,L_{1-2}}\left(\frac{H\,s_{\tau5-6}\,s_{\tau3-4}}{L_{3-4}^{\,2}\,s_{\tau3-4}+H^2\,s_{\tau5-6}}\right)$
s_{1313}	$\frac{s_\tau}{4L}$	$\frac{s_\tau}{3\sqrt{3}L}$	$\frac{L_{1-2}}{2\,L_{3-4}}\left(\frac{H\,s_{\tau5-6}\,s_{\tau1-2}}{L_{1-2}^{\,2}\,s_{\tau1-2}+H^2\,s_{\tau5-6}}\right)$
s_{1212}	$\frac{s_\tau}{4L}$	$\frac{s_\tau}{3\sqrt{3}L}$	$\frac{L_{1-2}}{2H}\left(\frac{L_{3-4}\,s_{\tau3-4}\,s_{\tau1-2}}{L_{3-4}^{\,2}\,s_{\tau3-4}+L_{1-2}^{\,2}\,s_{\tau1-2}}\right)$

*foam cell reveals mechanical isotropy [10]

	d)	e)
s_{1111}	$\frac{\sqrt{3}\,(s_{nL}+3\,s_{\tau L})\,s_{nL}}{12\,H\,(s_{nL}+s_{\tau L})}$	$\frac{\sqrt{3}\,(3\,s_{nL}+2\,s_{\tau L})}{8\,H}$
s_{2222}	$\frac{\sqrt{3}\,(s_{nL}+3\,s_{\tau L})\,s_{nL}}{12\,H\,(s_{nL}+s_{\tau L})}$	$\frac{\sqrt{3}\,(3\,s_{nL}+2\,s_{\tau L})}{8\,H}$
s_{3333}	$\frac{2\sqrt{3}\,s_{nH}}{9L}$	$\frac{\sqrt{3}\,H\,s_{nH}}{3L^2}$
s_{1122}	$\frac{\sqrt{3}\,(s_{nL}-s_{\tau L})\,s_{nL}}{12\,H\,(s_{nL}+s_{\tau L})}$	$\frac{\sqrt{3}\,(s_{nL}-2\,s_{\tau L})}{8\,H}$
s_{1133}	0	0
s_{2323}	$\frac{2\sqrt{3}\,H\,s_{\tau H}\,s_{\tau L}}{3\,(3\,L^2\,s_{\tau L}+4\,H^2\,s_{\tau H})}$	$\frac{\sqrt{3}\,H\,s_{\tau H}\,s_{\tau L}}{(3\,L^2\,s_{\tau L}+2\,H^2\,s_{\tau H})}$
s_{1313}	$\frac{2\sqrt{3}\,H\,s_{\tau H}\,s_{\tau L}}{3\,(3\,L^2\,s_{\tau L}+4\,H^2\,s_{\tau H})}$	$\frac{\sqrt{3}\,H\,s_{\tau H}\,s_{\tau L}}{(3\,L^2\,s_{\tau L}+2\,H^2\,s_{\tau H})}$
s_{1212}	$\frac{\sqrt{3}\,s_{\tau L}\,s_{nL}}{6\,H\,(s_{nL}+s_{\tau L})}$	$\frac{\sqrt{3}\;s_{nL}}{8\,H}$

$S_{ijkl}=S_{ijkl}\left(s_{nL},s_{nH},s_{\tau L}\,s_{\tau H},L,H,.....\right)$

6. Appendix

Stiffness matrices for the considered types of symetry.

a) cubic symmetry:

$$\mathbf{S} = \begin{bmatrix} s_{1111} & s_{1133} & s_{1133} & 0 & 0 & 0 \\ s_{1133} & s_{1111} & s_{1133} & 0 & 0 & 0 \\ s_{1133} & s_{1133} & s_{1111} & 0 & 0 & 0 \\ 0 & 0 & 0 & 2s_{2323} & 0 & 0 \\ 0 & 0 & 0 & 0 & 2s_{2323} & 0 \\ 0 & 0 & 0 & 0 & 0 & 2s_{2323} \end{bmatrix}$$

b) isotropy:

$$\mathbf{S} = \begin{bmatrix} s_{1111} & s_{1122} & s_{1122} & 0 & 0 & 0 \\ s_{1122} & s_{1111} & s_{1122} & 0 & 0 & 0 \\ s_{1122} & s_{1122} & s_{1111} & 0 & 0 & 0 \\ 0 & 0 & 0 & s_{1111} - s_{1122} & 0 & 0 \\ 0 & 0 & 0 & 0 & s_{1111} - s_{1122} & 0 \\ 0 & 0 & 0 & 0 & 0 & s_{1111} - s_{1122} \end{bmatrix}$$

c) orthotropy:

$$\mathbf{S} = \begin{bmatrix} s_{1111} & s_{1122} & s_{1133} & 0 & 0 & 0 \\ s_{1133} & s_{2222} & s_{2233} & 0 & 0 & 0 \\ s_{1133} & s_{2233} & s_{3333} & 0 & 0 & 0 \\ 0 & 0 & 0 & 2s_{2323} & 0 & 0 \\ 0 & 0 & 0 & 0 & 2s_{1313} & 0 \\ 0 & 0 & 0 & 0 & 0 & 2s_{1212} \end{bmatrix}$$

d), e) transversal isotropy:

$$\mathbf{S} = \begin{bmatrix} s_{1111} & s_{1122} & s_{1133} & 0 & 0 & 0 \\ s_{1133} & s_{1111} & s_{1133} & 0 & 0 & 0 \\ s_{1133} & s_{1133} & s_{3333} & 0 & 0 & 0 \\ 0 & 0 & 0 & 2s_{2323} & 0 & 0 \\ 0 & 0 & 0 & 0 & 2s_{2323} & 0 \\ 0 & 0 & 0 & 0 & 0 & s_{1111} - s_{1122} \end{bmatrix}$$

REFERENCES

[1] L.J. Gibson, M.F. Ashby, *Cellular Solids*, 2nd edition Cambridge University Press. (1997).

[2] J. Banhart, Manufacture, characterization and application of cellular metals and metal foams, Progress in Materials Science, 46, 559-632, (2001).

[3] A.G. Evans, J.W. Hutchinson, N.A. Fleck, M.F. Ashby, N.H. Wadley, The topological design of multifunctional cellular metals, Progress in Materials Science **46**, 309-327, (2001).

[4] O. Sigmund, Tailoring materials with prescribed elastic properties, Mech. Mat. **20**, 351-368. (1995).

[5] M.P. Bendsoe, J.M. Guedes, R.B. Haber, Petersen, J.E. Taylor, An analytical model to predict optimal material properties in the context of optimal structural design, J. Appl. Mech. **61**, 930-937, (1995).

[6] M.P. Bendsoe, A.R. Diaz, R. Lipton, J.E. Taylor, Optimal design of material properties and material distribution for multiple loading cases, Int. J. Num. Meth. Engn **38**, 1149-1170, (1995).

[7] M. Hori, S. Nemat-Nasser, On micromechanics theories for determining micro-macro relations in heterogeneous solids, Mech. Mat. **31**, 667-682, (1999).

[8] S. Nemat-Naser, M. Hori, *Micromechanics*,. 2nd edition Elsevier 1999.

[9] R. Philips, Crystals, Defects and Microstuctures. Modeling across Scales, Cambridge U.K. Cambridge University Press (2001).

[10] M. Janus-Michalska, R.B. Pęcherski, Macroscopic properties of open-cell foams based on micromechanical modelling, Technische Mechanik, Band **23**, 2-4 (2003).

[11] M.M. Mehrabadi, S.C. Cowin, Eigentensors of linear anisotropic elastic materials, Q. J. Mech. Appl. Math. **43**, 15-41 (1990).

[12] J. Rychlewski, Unconventional approach to linear elasticity, Arch. Mech. **47**, 149-171. (1995).

[13] S.C. Cowin. On the number of distinct elastic constants associated with certain anisotropic symmetries, Z. Angew. Math. Phys. **46**, 210-224 (1995).

[14] J. Ostrowska-Maciejewska, J. Rychlewski, Generalized proper states for anisotropic elastic materials, Arch. Mech. **53** (4-5), 501-518 (2001).

[15] T. Bohlke, C. Briiggemann, Graphical representation of the generalized Hooke's law, Technische Mechanik, Band **21**, 2, 145-158 (2001).

[16] A. Cazzani, M. Rovati, Extrema of Young modulus for cubic and transversely isotropic solids, Int. Journ. of Solids and Struct. **40**, 1713-1744 (2003).

[17] M. Hayes, A. Schuvalov, On the extreme values of Young modulus, the shear modulus and Poisson's ratio for cubic materials, ASME Journ. Appl. Mech. **65**, 786-787 (1988).

[18] J. Ostrowska-Maciejewska, J. Rychlewski, Generalized proper states for anisotropic elastic materials, Arch. Mech. **53**, (4-5), 501-518 (2001).

[19] D.W. Overaker, A.M. Cuitino, N.A. Langrana, Elastoplastic micromechanical modeling of two dimensional irregular convex and nonconvex hexagonal foams **65**, J. Appl. Mech. 748-757 (1998).

Received: 10 May 2005.